Preparation of Tricalcium phosphate: effect of precursor addition rate on the microstructural properties

A. Massit[1], A. El Yacoubi[1], A. Rezzouk[2], B. Chafik El Idrissi[1]

#1 Team materials surfaces interfaces, laboratory materials and energitics, fac of science, University Ibn Tofail, kenitra, Morocco.
#2 LPS, Fac. des sciences Dhar El Mehraz, BP 1796, Atlas FES, Morocco

ABSTRACT

The effect of the wet chemical method mixture precipitation and the precursor addition rate control of mixture solution on the fabrication and microstructural properties of β-tricalcium phosphate (β-TCP; $Ca_3(PO_4)_2$) powders was examined. The β-tricalcium phosphate powders with high purity could be attained through mixing and precipitating $(NH_4)_2HPO_4$ and $Ca(NO_3)_2.4H_2O$ with solution state and controlling the addition rate of mixture solution in varying a precursor addition rate 300ml/min, 30ml/min and 3ml/min. The X-ray Diffraction (XRD) analysis results showed that the peak of calcium pyrophosphate ($Ca_2P_2O_7$) excluding the peaks associated with β-tricalcium phosphate was appeared at slow addition of precursor (30 and 3 ml/min) but it was not appeared at the maximum flow rate (300 ml/min), the observed Fourier Transform Infrared Spectroscopy (FT-IR) results showed that a presence of a trace amount of β-$Ca_2P_2O_7$ undetectable by XRD. The crystallite size of precipitated β-tricalcium phosphate powders, calculated by XRD method, is 40 nm (300ml/min) and 56 nm (30ml/min).

.

Key words: β-tricalcium phosphate; Wet precipitation; precursor addition rate control; Phase purity; crystallite size

Corresponding Author: B. Chafik El Idrissi: chidrissi@yahoo.fr

1. INTRODUCTION

The application of calcium phosphate ceramics has become relatively to far and wide in the biomedical materials field, due to their biocompatibility with human hard tissue [1-5]. Of theses, the β-tricalcium phosphate (β-TCP), represented by the chemical formula of $Ca_3(PO_4)_2$ with Ca/P ratio of 1.5, has received great attention as grafts for bone regeneration applications due to its excellent biocompatibility and biodegradability [6]. TCP can also be utilized as a precursor for the preparation of apatites [7,8]. The solubility of β-TCP into water is about twice as high as that of hydroxyapatite (HA) $Ca_{10}(PO_4)_6(OH)_2$ [9]. Therefore, the various methods such as solid-state reactions, wet precipitation, sol-gel methods, and hydrothermal treatment [10-12] to synthesize it

have been developed. Particularly, the wet precipitation processing has mostly been used due to a low cost and a better control of composition and physical properties of powders [13]. This method usually results in the formation of a non-stoichiometric apatite whose molar ratio of Ca/P is from 1.33 to 1.65 [14-19]. Non-stoichiometric apatite with formula $Ca_{10-x}(HPO_4)_x(PO4)_{6-x}(OH)_{2-x}$ ($0 \leq x \leq 1$) exhibits the same crystal structure as stoichiometric HA. When Ca/P molar ratio is equal to 1.5, corresponding to x = 1 in the above-mentioned formula, the $Ca_9(HPO_4)(PO_4)_5(OH)$ is called tricalcium phosphate apatite (ap-TCP), which has an apatite crystal structure and the molar ratio of Ca/P is equal to TCP (Ca/P=1.5). Conventionally, ap-TCP powders are synthesized via a wet chemical method as described by the following equation Eq. (1).

$$9Ca(NO_3)_2 + 6(NH_4)_2HPO_4 + 6NH_4OH \rightarrow Ca_9(HPO_4)(PO_4)_5OH + 18NH_4NO_3 + 5H_2O \quad (1)$$

When the ap-TCP was calcined above 700–800°C, it will be transformed into β-TCP, as described by Eq. (2).

$$Ca_9(HPO_4)(PO_4)_5OH \rightarrow Ca_9(PO_4)_6H_2O \rightarrow 3\ Ca_3(PO_4)_2 + H_2O \quad (2)$$

Specific characteristics of particles (size, shape, surface, crystal structure and morphology) are among the important factors needed to control technological and biopharmaceutical properties of drug products. In general, morphology can influence the physical and chemistry stability of solid dosage forms, a narrow size distribution is important to obtain content uniformity, while spherical particles allow good flowability and tablettability. Furthermore, micronisation increases the surface area with a consequent increase of dissolution rate and bioavalability of the drug, thus promoting the formulation of active principle ingredients which may be insoluble or slightly soluble in aqueous media. Bioactivity of calcium phosphate materials depends on many factors during the synthesis procedure including precursor reagents, impurity contents, crystal size and morphology, concentration and mixture order of reagents, pH and temperature. Such conditions are application specific and should be controlled by synthesis preparation parameters [20, 21].

The main objective of the present work is to study the effect of the wet chemical method and the precursor addition rate on the phase purity of the β-tricalcium and the microstructural properties. We also verified the phase purity and the microstructure of the precipitated β-tricalcium phosphate powders by using Fourier Transform Infrared Spectroscopy (FT-IR), X-ray Diffraction (XRD) and Transmission Electron Microscopy (TEM).

2. EXPERIMENTAL

2.1. Powder synthesis

Reaction condition for the preparation of β-TCP using wet chemical method was initially optimized. Analytical grade calcium nitrate tetrahydrate [$Ca(NO_3)_2 \cdot 4H_2O$] and diammonium hydrogen phosphate [$(NH_4)_2HPO_4$] were dissolved in distilled water, individually. The $Ca(NO_3)_2 \cdot 4H_2O$ solution was added drop-wise (under a constant stirring condition at ambient temperature), at different precursor addition rate 300 ml/min, 30 ml/min and 3 ml/min, into $(NH_4)_2HPO_4$ solution to reach the Ca/P molar ratio of 1.5. The pH was adjusted throughout by the addition of concentrated ammonium hydroxide (NH_4OH) solution to around 9.5. The resulting precipitates were aged for 48 h under stirring before being filtered and washed repeatedly by distilled water to remove NO_3^- and NH_4^+. Then, the precipitates were dried at 60°C for 24 h. The calcium-deficient apatite precipitates were produced. These precipitated

powders were calcined at 800˚C for 12 hrs to transform from tricalcium phosphate apatite to β-tricalcium phosphate.

2.2. Characterization of the powders

Crystalline phases were identified by means of a XPERT-PROPW3050/60 (Theta/Theta) X-ray diffractometer (XRD) using CuKα radiation and operating at 45 kV and 40 mA. XRD patterns were collected over the 2θ range of 3-70° at a step size of 0.06°. Crystalline phases detected in the patterns were identified by comparison to the standard patterns from the ICDD-PDF (International Center for Diffraction Data-Powder Diffraction Files). The functional groups present in the prepared powder were recorded on FTIR spectrophotometer, VERTEX 70, Genesis Series (400–4000 cm-1, resolution 4, scans 20). For this 1% of the powder was mixed and ground with 99% KBr and the spectrum was taken in the range of 400 to 4000 cm^{-1}. The size and morphology of fine powders were observed on a transmission electron microscope (Philips CM10, Eindhoven, The Netherlands) that operated at the acceleration voltage of 100 kV.

3. RESULTS AND DISCUSSION

The XRD patterns for the three precipitates dried at 60 °C for 24 h are shown in Fig. 1. Similar XRD patterns are obtained for these powders and exhibit two distinguishable crystalline phases can be indexed as tricalcium phosphate apatite and a second phase identified as dicalcium phosphate anhydrous $CaHPO_4$ (DCPA, PDF 9–80). These results should be in better agreement with an initial precipitation of $CaHPO_4,2H_2O$ DCPD followed by its slow and partial hydrolysis into apatitic tricalcium phosphate and would explain that the final mixture contains dicalcium phosphate anhydrous $CaHPO_4$ as a second phase after drying [22]. The presence of $CaHPO_4$ phase is confirmed by two intense peaks at 26.24° and 29.98°.

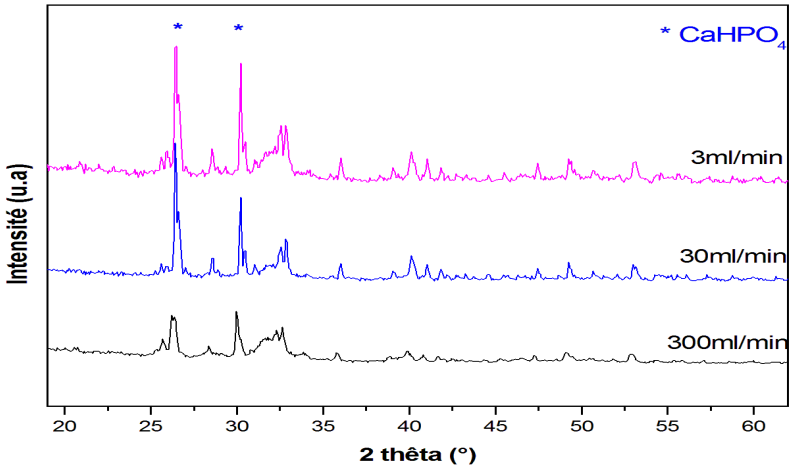

Fig 1: XRD patterns of dried samples at 60°C

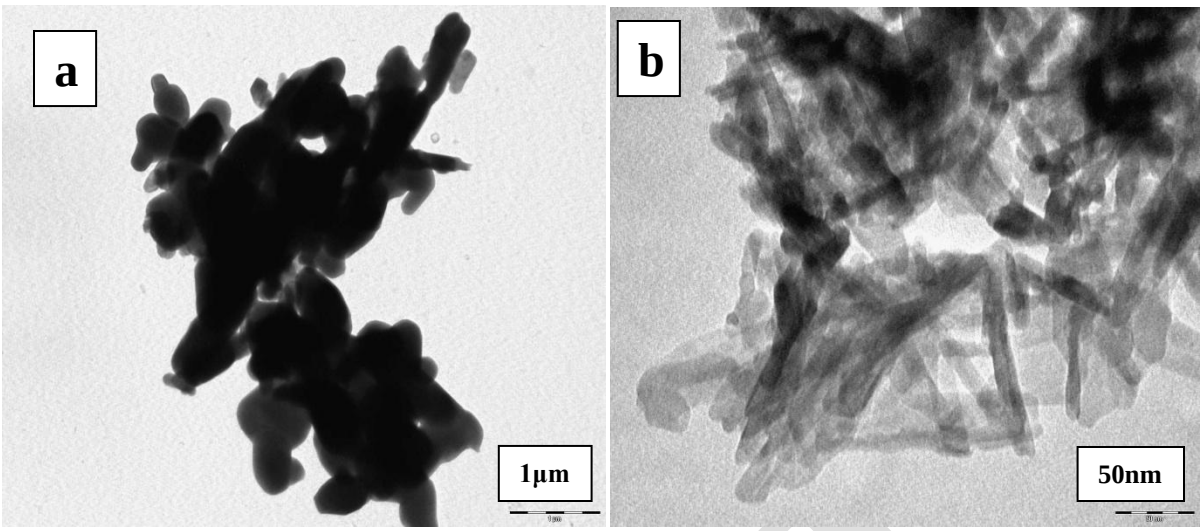

Fig 2: TEM micrograph of synthetic powders at 60°C with 30ml/min (a), 300ml/min (b)

The needle-like particles can be observed by transmission electron microscopy as shown in Fig. 2(a), of synthetic powder with 300ml/min, and are rather similar to that of tricalcium phosphate apatite synthesized by wet-chemical processing [18,19,23], the morphology exhibits needle-like structure with 10 nm in width and 30–40 nm in length. Fig. 2(b) presents that TEM morphology of powders synthesized with 3ml/l. The structures are spherical rod-like and are about 180 nm in diameter and 400-500 nm in length. With the increase of precursor addition rate, it can be observed that the needle- like nanostructure transformed into a spherical rod-like nanostructure and its aspect ratio decreased.

Fig. 3 illustrates the FT-IR absorption spectra of the as-dried samples. The bands at 1092 and 1040 cm^{-1} are assigned to the components of the triply degenerate ν3 antisymmetric P–O stretching mode. The 962 cm^{-1} band is assigned to ν1; the non-degenerate P–O symmetric stretching mode. The bands at 601 and 571 cm^{-1} are assigned to components of the triply degenerate ν4 O–P–O bending mode. Molecular and adsorbed water bands are also discerned at 1640 and 3400 cm^{-1}. A significant concentration of hydroxyl groups remains in the structure as observed from the intensity of the stretching and librational bands at 3572 and 632 cm^{-1}. In addition, the band at 1380 cm^{-1} assigned to NH_4OH and NO_3^-. A weak band near 875 cm^{-1} is possible the P–O(H) stretching in HPO_4^{2-} groups or ν2 vibration mode of CO_3^{2-} groups. However, no ν3 vibration mode (near 1490 and 1426 cm^{-1}) of CO_3^{2-} groups was observed in the FT-IR spectra. Therefore, it was believed that the weak peak at 875 cm^{-1} was primarily characteristic of the HPO_4^{2-} although CO_2 has a very affinity to apatite crystal during the synthesis process.

The phase transformation from ap-TCP to β-TCP was performed by heating the samples at 800°C. Fig. 4 shows the XRD patterns of samples after calcinations at 800°C, all the diffraction peaks positions match well with the standard XRD pattern of β-TCP (JCPDS NO.9-169). Powders exhibited sharp diffraction peaks indicating a high crystallinity. The pattern for sample TCP300 (prepared with a precursor addition rate 300 ml/min) shows well characterized peaks of pure β-TCP. The diffractograms of the samples TCP30 and TCP3 (prepared with a precursor addition rate 30 ml/min and 3 ml/min respectively) show additional peaks rather than the β-TCP peaks.

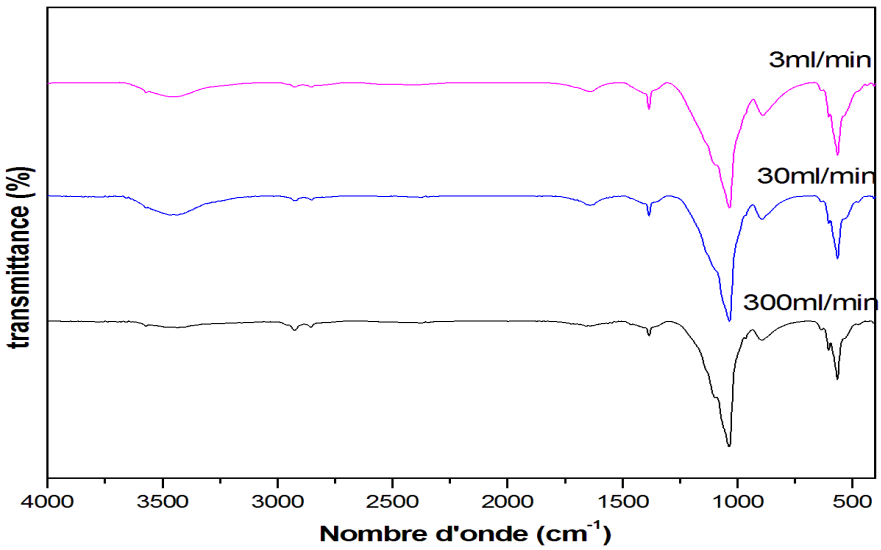

Fig 3: FT-IR spectra of dried samples at 60°C

The peaks were identified to be corresponding to pyrophosphate β-$Ca_2P_2O_7$ (CPP) and indexed according to the standard value (JCPDF 9-346).

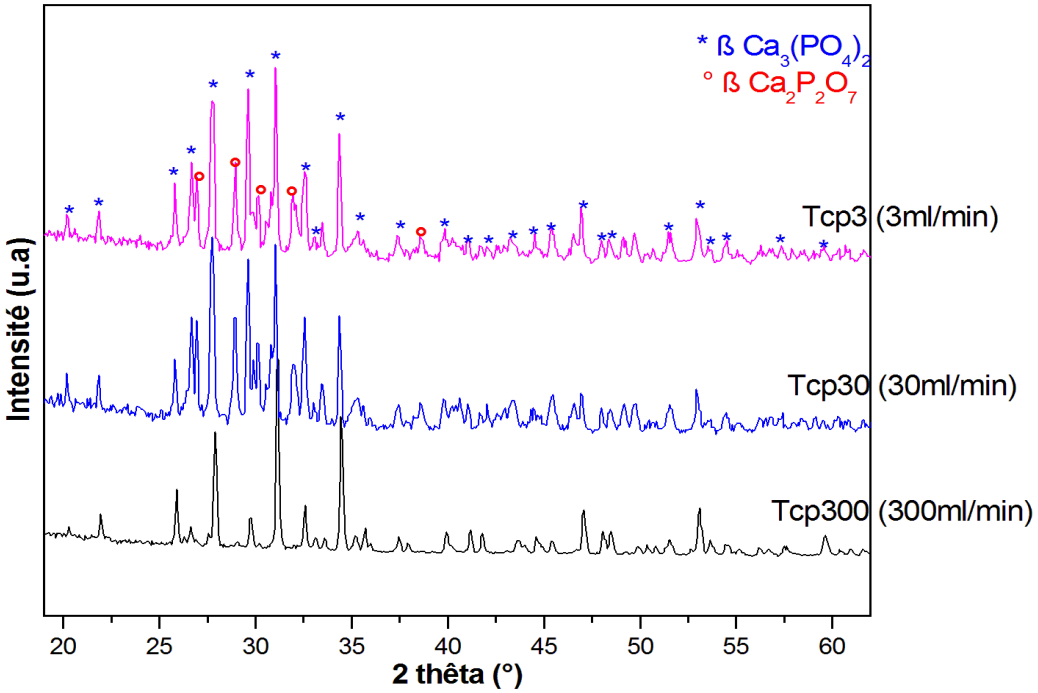

Fig 4: XRD patterns of samples calcined at 800°C

This second phase associated with the transformation of DCPA into β-CPP according to [24]:
$2CaHPO_4 \rightarrow (\delta)\ Ca_2P_2O_7 + H_2O$ (450°C)
$(\delta)\ Ca_2P_2O_7 \rightarrow (\beta)\ Ca_2P_2O_7$ (750°C)
The percentages of volume fraction of β-CPP and β-TCP present in the samples were calculated using the relative intensity ratio (RIR), Eq. (3) [25]. The ratio of the integrated intensity of the (2 0 2) diffraction peak of β -CPP to the integrated intensity of the (0 2 10) diffraction peak of β -TCP was calculated. The (2 0 2) peak at 2θ = 28.9° of CPP was the most intense usable peak for the quantification (relative intensity 45%). RIR = 33% and 34% for TCP30 and TCP3 respectively.

$$RIR = \boldsymbol{I}_{\beta\text{-CPP}} / \boldsymbol{I}_{\beta\text{-CPP}} + \boldsymbol{I}_{\beta\text{-TCP}} \quad (3)$$

Where $\boldsymbol{I}_{\beta\text{-CPP}}$ and $\boldsymbol{I}_{\beta\text{-TCP}}$ represent the normalized intensity of (2 0 2) and (0 2 10) peaks of β-CPP and β-TCP respectively.
The crystallinity degree, corresponding to the fraction of crystalline β-TCP phase present in the examined volume, was evaluated by (Xc) by the following Eq. (4) [26]:

$$Xc = 1 - \nu/I \quad (4)$$

Where I is the intensity of highest diffraction peak and ν is the intensity of the hollow between two considered diffraction peaks of β-TCP. Table 1 shows the amount of crystallinity in TCP powders. The crystallization process is controlled by diffusion. It seems that by using wet chemical method increasing precursor addition rate influences the rate of atomic motion and decreases the diffusion barrier. So the atoms are easily transported to the lattice site and the crystallinity is increased.

Table1. The effect of addition rate on crystallinity, crystallite size and particle size

Sample	*amount of crystallinity (%Xc)*	*Crystallite size (nm)*	*Particle size (nm)*
TCP3	72	56	-
TCP30	75	54	130-300
TCP300	93	40	80-200

The broadening of a diffraction peak can be related to the crystallite size via the Scherer equation relying on Eq. (5).

$$D = 0.89\ \lambda / \beta \cos\theta \quad (5)$$

Where D the mean crystallite size, λ is the wavelength of the used Cu Kα radiation, β is the full width at the half maximum of the β-TCP line and θ is the diffraction angle. The crystallite sizes of β-tricalcium phosphate are given in Table 1. These results clearly indicate that using wet chemical method and increasing precursor addition rate result in increasing crystallite size of the powders.
The transmission electron microscope of TCP30 and TCP300 powders are illustrated in Fig. 5. They demonstrate many agglomerations of small spherical particles in nanometric scale. The grain size measurement reveals that the grain size of TCP30 powders is around 120 nm to 300 nm and the grain size of TCP300 powders is around 80–220 nm. By varying the precursor addition rate, nucleation and crystal growth rates can be controlled, rapid addition of precursors results in localized high concentrations of precursors, exceeding the solubility of TCP in those regions, which favors nucleation and formation of small crystals. Slow addition of precursors results in a regime favoring crystal growth and formation of larger particles.

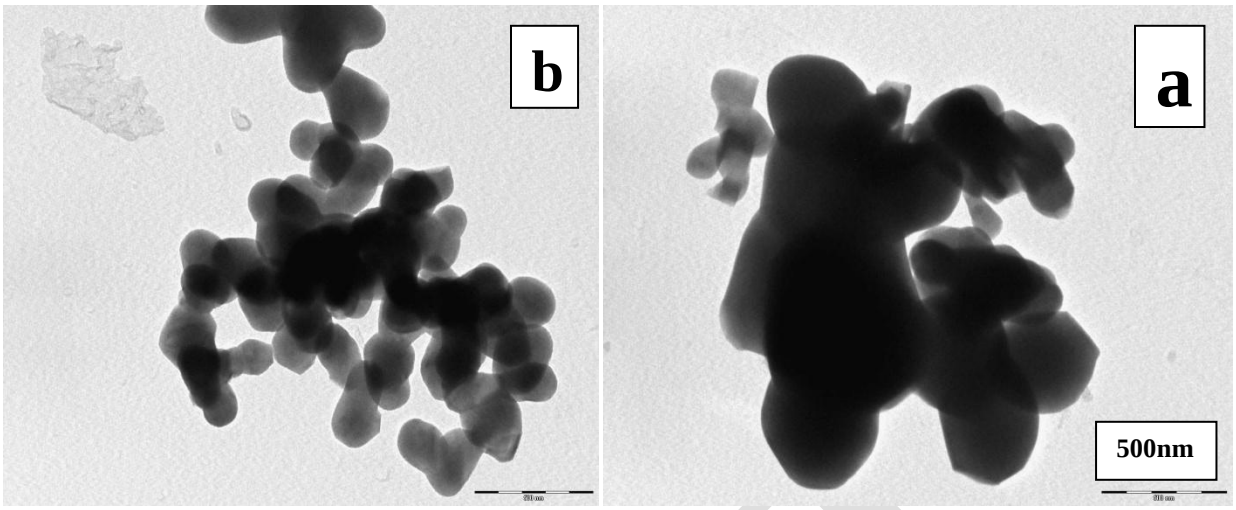

Fig 5: TEM micrograph of calcined powders at 800°C with 30ml/min (a), 300ml/min (b)

Fig. 6 gives the IR spectra of powders heat-treated at 800°C. They agree with the phases determined from XRD patterns of calcined powders. The vibrational bands of the phosphate ions are observed in all of the samples. The band attributed to HPO_4 groups in the as synthesized and dried at 60°C powder (v = 875 cm^{-1}) had disappeared. This corresponds with the decomposition of tricalcium phosphate apatite that occurs around 750°C according to the global reaction as described by the Eq. (2). The band assigned to OH group (630 cm^{-1}) had disappeared at 800°C, and the PO4 bands are present on account of the decomposition of the apatitic phase into β -TCP. The bands at 725 and 1200 cm^{-1} indicated the presence of P_2O_7 groups associated with the transformation of DCPA into CPP. There is insignificant amount of β-$Ca_2P_2O_7$ in TCP300 undetectable by XRD.

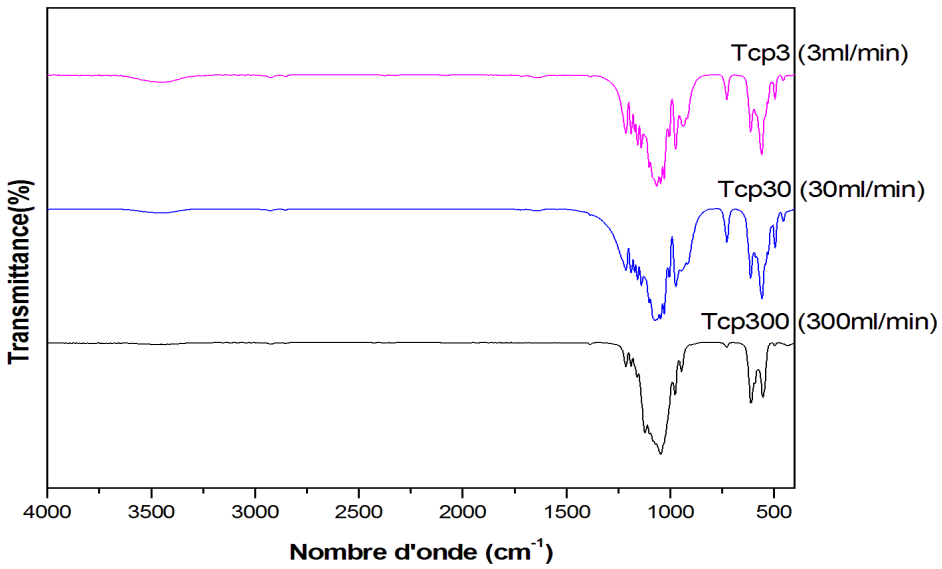

Fig 6: FT-IR spectra of samples calcined at 800°C

CONCLUSION

Nano-crystalline TCP can be synthesized by chemical precipitation method followed by calcinations at 800°C. The effects of precursor addition rate (P.A.R) on the crystallite size, particle size and the crystallinity can be examined. P.A.R affects the nucleation, crystal growth rates and particle morphology. The nano-tricalcium phosphate powder, synthesized at the maximum flow rate, givens an ultrafine crystal size of about 40 nm and spherical particle size distributions with an average around 80 nm to 200 nm. At the minimum flow rate (30ml/min), crystallite size greater than about 60 nm, an average particle size of 130 nm to 300 nm. From FTIR and XRD, the calcined powders present a second phase identified as pyrophosphate β-CPP.

REFERENCE

[1] Y. Li, Klein CPAT, J. Wijn, S. Meer, K. Groot. J Mater Sci Mater Med 1994;5:263-8.
[2] IH. Arita, VM. Castano, DS. Wilkinson. J Mater Sci Mater Med 1995;6:19-23.
[3] D. Liu. Ceram Int 1997;23:135-9.
[4] CA Tas, F. Korkusuz, M. Tumucin, N. Akkas. J Mater Sci Mater Med 1997;8:91-6.
[5] R. Rao, HN. Roopa, TS. Kannan. J Mater Sci Mater Med 1997;8:511-8.
[6] F. Zhang, K. Lin, J. Chang, J. Lu, C. Ning. J Eur Ceram Soc 2008;28:539-45.
[7] B.V. Rejda, J.G.J. Peelen, K. de Groot, J. Bioeng. 1 (1977) 93–97.
[8] A. Bigi, L. Compostella, A.M. Fichera, E. Foresti, M. Gazzano, A. Ripamonti, N. Roveri, J. Inorg. Biochem. 34 (1988) 75–82.
[9] A. Makishima, H. Aoki, in: T. Yamaguchi, H. Yanagida (Eds.), Bioceramics, Giho-do Pub. Co., Tokyo, 1984, p. 28.
[10] M. Bohner. Injury-Int J Care Injured 2000;31:S-D37-47.
[11] M. Vallet-Regí, JM. González-Calbet. Prog Solid State Chem 2004;32:1-31.
[12] M. Fathi, A. El Yacoubi, A. Massit, B. Chafik El Idrissi. IJSER Volume 6, Issue 6, June-2015;139-143.
[13] DRR. Lazar, SM. Cunha, V. Ussui, E. Fancio, NB. de Lima, AHA. Bressiani. Mater Sci Forum 2006;530-531:612-7.
[14] L. Yubao, Klein CPAT, Z. Xingdong, K. de Groot. ceramics. Biomaterials 1994;15:835–41.
[15] A. Slosarczyk, E. Stobierska, Z. Paszkiewicz, M. Gawlicki. J Am Ceram Soc 1996; 79(10): 2539–44.
[16] TSB. Narasaraju, DE. Phebe. J Mater Sci 1996;31:1–21.
[17] M. Vallet-Regi, LM. Rodriguez-Lorenzo, AJ. Salinas. Solid State Ionic 1997;101–103: 1279–85.
[18] A. Massit, A. El Yacoubi, B. Chafik El Idrissi, K. Yamni. IOSR-JAC. Volume 7, Issue 7 Ver. I. (July. 2014), PP 57-61.
[19] A. Massit, A. Yacoubi, B. Chafik El Idrissi, K. Yamni. Verres, Céramiques & Composites, Vol. 4, N°1 (2015), 1-6.
[20] M. Santos, M. Oliveira, L. Souza, H. Mansur, W. Vasconcelos, Materials Research 7 (2004) 625–630
[21] A. Farzadi, M. Solati-Hashjin, F. Bakhshi, A. Aminian. Ceramics International 37 (2011) 65–71
[22] A. Destainville, E. Champion, D. Bernache-Assollant, E. Laborde. Materials Chemistry and Physics 80 (2003) 269–277

[23] A. El Yacoubi, A. Massit, M. Fathi, B. Chafik El Idrissi. IJOART, Volume 4, Issue 7, July - 2015
[24] Jo Duncan, James F. MacDonald, JohnV.Hanna, YukiShirosaki, Satoshi Hayakawa, Akiyoshi Osaka, Janet M.S. Skakle, Iain R. Gibson. Materials Science and Engineering C 34 (2014) 123–129
[25] E.C. Victoria, F.D. Gnanam, Trends in Biomaterials and Artificial Organs 16 (2002) 12–14.
[26] E. Landi, A. Tampieri, G. Celotti, S. Sprio, J. Eur. Ceram. Soc. 20 (2000) 2377–2387.